DESIGNING AND VERIFYING THE OUTER CASING OF AN EXTERNAL COMBUSTION STIRLING ENGINE THROUGH FINITE ELEMENT ANALYSIS

Dănuț-Iulian Stanciu[1,][0000-0002-2160-6955], Oleg Krol[2][000-0003-0193-2750] and Vladimir Sokolov [2][0000-0003-0459-1824]*
[1]National Institute of Research and Development in Mechatronics and Measurement Technique – INCDMTM, Șos. Pantelimon, nr. 6-8, sector 2, Bucharest, Romania
[2]Volodymyr Dahl East Ukrainian National University: 17 Ioanna Pavla II str., Kyiv 01042, UA
E-mails: danut.stanciu@incdmtm.ro, krolos@i.ua*

Abstract - Stirling engines are external combustion engines that have recently attracted the attention of researchers due to their ability to use renewable heat sources (solar, geothermal, biomass, etc.). One drawback of these engines is that they have a low power-to-weight ratio, and one way to increase this ratio is to increase the average working pressure of the working gas, which leads to increased stresses on the outer casing of the engine, which must then be dimensioned to be safe in operation. This article presents a method for designing and verifying the outer casing of an external combustion Stirling engine through finite element analysis using the open-source Code-Aster / Salome-Meca calculation program.

Keywords: Finite element, Stirling engine, Open source, Salome-Meca.

1. Introduction

The Stirling engine is an external combustion heat engine that converts thermal energy into mechanical work through cyclic compression and expansion of a working gas (typically helium, hydrogen, or air).

One of the key factors determining its performance is the mean working gas pressure.

In practical implementations, most Stirling engines operate at or near atmospheric pressure, limiting the maximum indicated power.

The image of the studied Stirling Engine (gamma model) realized in project "New Techniques and Methods for the Manufacture of Solar Thermal Systems with Flat-Plate Concentrators Using Additive Manufacturing Methods" as an experimental model is presented in figure 1.

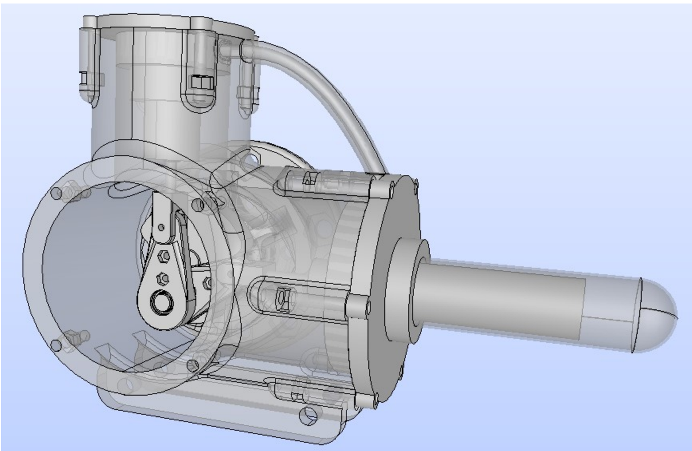

Figure 1: Gamma Stirling engine

https://doi.org/10.17683/ijomam/issue22.v2.20

Previous studies (e.g., Walker [11]; Senft[12]) have shown that increasing the mean gas pressure increases the **mass of working gas** enclosed in the cycle, resulting in higher work per cycle. However, the mechanical implications of increased pressure on the engine structure (especially the **Carter crankcase** and **displacer cylinder**) must be verified to ensure safe operation.

This study provides:

1. A theoretical proof that Stirling engine power scales with mean pressure.
2. A proposal to validate the mechanical safety of the Carter engine under pressure using **Salome-Meca finite element analysis (FEA)**.

2. Theoretical Background

2.1. Ideal Stirling Cycle Work

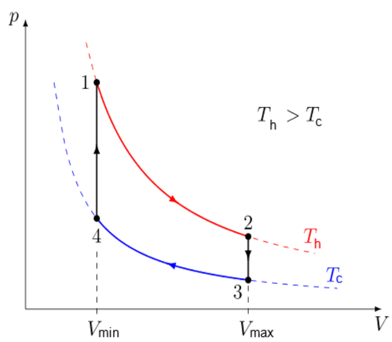

Figure 2: Ideal Stirling cycle

The ideal Stirling cycle consists of four processes:

1. Isothermal expansion at the hot temperature Th, from Vmin to Vmax.
2. Isochoric (constant-volume) cooling from Th to Tc.
3. Isothermal compression at the cold temperature Tc from Vmax back to Vmin
4. Isochoric heating back to Th

Only the isothermal processes (1) and (3) perform net work.

The constant-volume steps exchange heat but do not contribute to the total mechanical work.

For an ideal gas under isothermal expansion or compression:

Energy for a gas

$$W = nRT ln\left(\frac{V_{final}}{V_{initial}}\right) \quad (1)$$

where:

n - is the number of moles of gas

R - the gas constant,

Th and Tc - the hot and cold temperatures,

Vmax, Vmin - the maximum and minimum volumes of the engine.

So, for the two active branches:

Expansion at Th:

$$W_{exp} = nRT_h \ln\left(\frac{V_{max}}{V_{min}}\right) \quad (2)$$

Compression at Tc

$$W_{comp} = nRT_c \ln\left(\frac{V_{min}}{V_{max}}\right) = -nRT_c \ln\left(\frac{V_{max}}{V_{min}}\right) \quad (3)$$

Net Work per Cycle

Adding the two:

$$W_{net} = W_{exp} + W_{comp} = nR\,(T_h - T_c)\ln\left(\frac{V_{max}}{V_{min}}\right) \quad (4)$$

In conclusion

For an ideal Stirling engine, the work per cycle is given by:

$$W = nR(T_h - T_c)\ln\left(\frac{V_{max}}{V_{min}}\right) \quad (5)$$

The mean pressure is related to the total mass of gas by:

$$P_m = \frac{nRT_{mean}}{V_{mean}} \quad (6)$$

Thus, for a fixed geometry and temperature range energy is proportional with pressure:

$$W \propto P_m \quad (7)$$

and since the power P is W × f (frequency), then:

$$P_{out} \propto P_m \quad (8)$$

This shows that **increasing mean pressure directly increases mechanical power output**, assuming the same cycle speed and temperatures, thus for increase the power of a Stirling Engine is sufficient to increase the mean working pressure. Increasing working pressure means that external case of the engine needs to be designed to resists of the working pressure.

Simple case forms could be made by formula calculation but for complicated case forms (as Stirling Engine case) the results could be obtained only by finite element analysis.

3. Experimental and Simulation Methodology

3.1. Pressure-Assisted Operation

To experimentally or numerically simulate a pressurized Stirling engine, the entire working chamber and crankcase can be placed in a sealed enclosure filled with a gas at a controlled pressure (e.g., 1–10 bar). The purpose is to increase the mean gas density without altering geometry.

3.2. Mechanical Verification Using Salome-Meca

To verify the Carter-type Stirling engine under supplementary pressure, the following **finite element analysis (FEA)** procedure is proposed:

3D CAD Model:

Import the Carter mechanism geometry (crankcase, cylinder, piston) into **Salome-Meca.**

Material Definition:

Define materials of the enclosure (plastic resin used in 3D printer):

Table 1: Tensile Properties

	Green	Post Cured
Ultimate Tensile Strength	38 MPa	65 MPa
Tensile Modulus	1.6 GPa	2.8 GPa
Elongation at Break	12%	6%

Boundary Conditions:

- Apply internal pressure P_{test}=1...10 bar on all surfaces in contact with the gas.
- Fix crankshaft bearing supports.
- Constrain symmetry if possible to reduce computation time.
- **Meshing:**
  Use tetrahedral second-order mesh (NETGEN 1.2) with refinement in thin wall regions.

Solver Setup:

- Use **Code_Aster** under **MECA_STATIQUE** analysis to compute:
- Maximum von Mises stress
- Total deformation
- Safety factor $SF = \frac{\sigma_{yield}}{\sigma_{max}}$ (9)

Verification Criterion:

Mechanical integrity is verified if SF >1.5 under maximum intended pressure.

4. Effective Simulation

4.1 Testing the finite element analysis method of Salome-Meca software.

In order to compare the stress results applied to a closed enclosure filled with pressurized gas (air) obtained by the Salome-Meca software, a stress test will first be performed on a thick-walled tube containing pressurized air, for which the formula for calculating the total stress is known. The results obtained will be compared with the theoretical results applied to the same tube.

Tube characteristic

D_{inner} = 400 mm
D_{outer} = 520 mm
Young's modulus = 210 GPa
Poissons ratio = 0.25

4.1.1 Theoretic Calculation

The pressure inside a thick-walled tube filled with a pressurized gas is given by the formula:

$$\sigma_{r,t}(r) = \frac{p_i \cdot R_i^2}{R_e^2 - R_i^2} \pm \frac{(-p_i)}{r^2} \cdot \frac{R_i^2 \cdot R_e^2}{R_e^2 - R_i^2} \quad (10)$$

where:

p_i – internal pressure
r - radius at which the tension is calculated
R_i – inner radius of the tube
R_e – outer radius of the tube

Radial stresses have the following law of variation:

$$\sigma_r(r) = \frac{p_i \cdot R_i^2}{R_e^2 - R_i^2}\left(1 - \frac{R_e^2}{r^2}\right) \quad (11)$$

and the tangential stresses have the following law of variation:

$$\sigma_t(r) = \frac{p_i \cdot R_i^2}{R_e^2 - R_i^2}\left(1 + \frac{R_e^2}{r^2}\right) \quad (12)$$

The maximum values of radial stress are given by the formula

$$\sigma_r(r) = \frac{p_i \cdot R_i^2}{R_e^2 - R_i^2}\left(1 - \frac{R_e^2}{R_i^2}\right) \quad (13)$$

(for r=R_i)

and the maximum values of the tangential stress are given by the formula

$$\sigma_t(r) = \frac{2 \cdot p_i \cdot R_i^2}{R_e^2 - R_i^2} \quad (14)$$

(for r=R_e)

From the graphs below, for the two categories of stress, it can be seen that the dangerous stress on the tube occurs on the inside, where the stress state is flat with the extreme principal stresses having opposite signs; in such cases, it is useful to calculate their overall effect using the τ_{max} rupture hypothesis, and the resistance calculation relationship is obtained as follows:

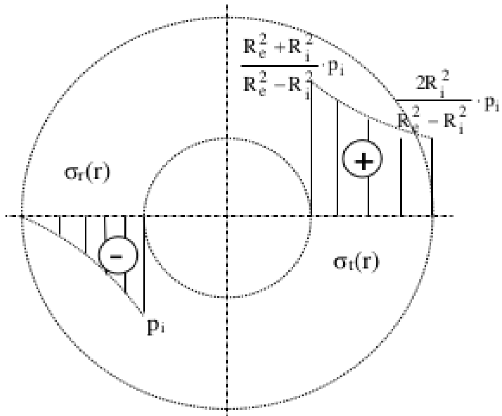

Figure 3: Radial and tangential tensions

$$\sigma_{echmax} = \frac{p_i \cdot R_e^i + R_i^2}{R_e^2 - R_i^2} + p_i = p_i \cdot \frac{2R_e^2}{R_e^2 - R_i^2} \quad (15)$$

By inserting the physical dimensions of the test tube (shown above) into formula [15], we obtain the maximum theoretical stress value:

$$\sigma = 97{,}97 MPa \quad (16)$$

4.1.2 Finite Element Simulation

To verify the accuracy of the calculation of the maximum stress of the thick-walled tube using the Salome-Meca program, the following steps were taken:

A 3D model of the thick-walled tube with the dimensions shown above was created (in the theoretical formulas, the tube is considered to be of infinite length; in the 3D model, we will use a length of 2 m). At the same time, the elements (surfaces) to be used in the simulation were created on the 3D model – the surfaces that will be fixed and the surface on which the pressure will be applied, and the grid used for the finite element calculation was created (Fig. 4)

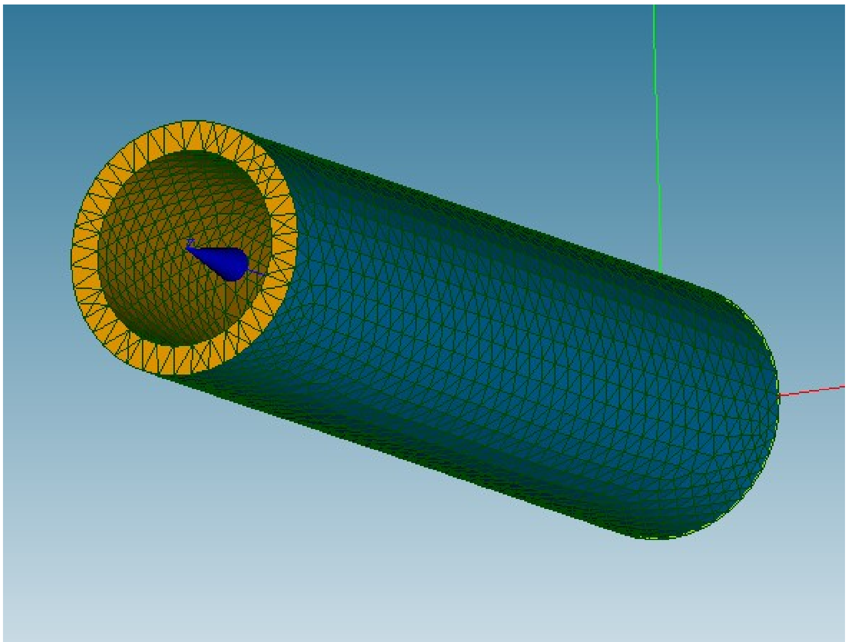

Figure 4: Discretization of thick-walled tube for finite element simulation of stress created by internal pressure

The characteristics of the network used for finite element calculation are shown in Figure 5.

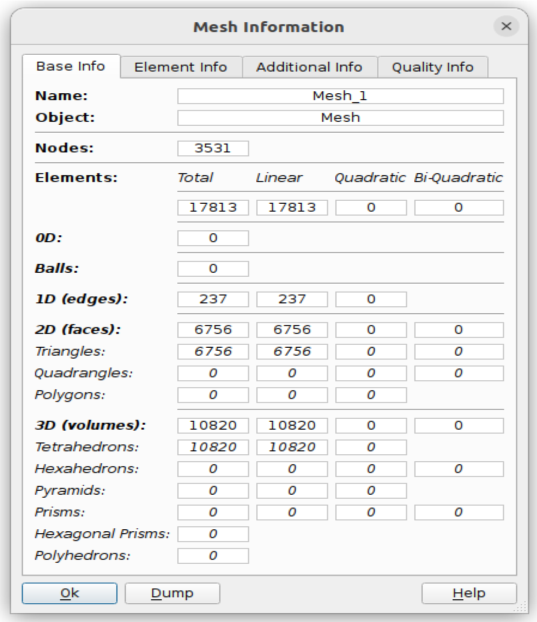

Figure 5: Mesh characteristics of the tested tube

A Code-Aster study is being conducted with the following components:

```
mesh = LIRE_MAILLAGE(
 FORMAT='MED',
 UNITE=20
)
 model = AFFE_MODELE(
 AFFE=_F(
  MODELISATION=('3D', ),
  PHENOMENE='MECANIQUE',
  TOUT='OUI'
 ),
 MAILLAGE=mesh
)
 mater = DEFI_MATERIAU(
 ELAS=_F(
  E=210000000000.0,
  NU=0.3
 )
)
 materfl = AFFE_MATERIAU(
 AFFE=_F(
  MATER=(mater, ),
  TOUT='OUI'
 ),
 MODELE=model
)
 mecabc = AFFE_CHAR_MECA(
 DDL_IMPO=_F(
  DX=0.0,
  DY=0.0,
  DZ=0.0,
  GROUP_MA=('fix', )
 ),
```

```
 MODELE=model
)
   mecach = AFFE_CHAR_MECA(
 MODELE=model,
 PRES_REP=_F(
  GROUP_MA=('presiune', ),
  PRES=20000000.0
 )
)
   result = MECA_STATIQUE(
 CHAM_MATER=materfl,
 EXCIT=(_F(
   CHARGE=mecabc
  ), _F(
   CHARGE=mecach
  )),
 MODELE=model
)
   result = CALC_CHAMP(
 CHAM_MATER=materfl,
 CONTRAINTE=('SIGM_ELGA', 'SIGM_ELNO'),
 CRITERES=('SIEQ_ELGA', 'SIEQ_ELNO'),
 MODELE=model,
 RESULTAT=result,
 TOUT='OUI'
)
   IMPR_RESU(
 FORMAT='MED',
 RESU=_F(
  RESULTAT=result
 ),
 UNITE=80
)
```

We perform the request and view the verification result using the maximum and minimum display function for the imposed request. For the result, we will use the request composed according to the Von Mises criterion [16].

$$\sigma_v = \sqrt{\frac{1}{2}[(\sigma_{xx}-\sigma_{yy})^2+(\sigma_{yy}-\sigma_{zz})^2+(\sigma_{zz}-\sigma_{xx})^2]+3(\sigma_{xy}^2+\sigma+yz^2+\sigma_{zx}^2)} \qquad (16)$$

Where:

$\sigma_{xx}, \sigma_{yy}, \sigma_{zz}$ axial forces

$\sigma_{xy}, \sigma_{yz}, \sigma_{zz}$ tangential forces

We visualize the result of the stress, shown in Figure 6.

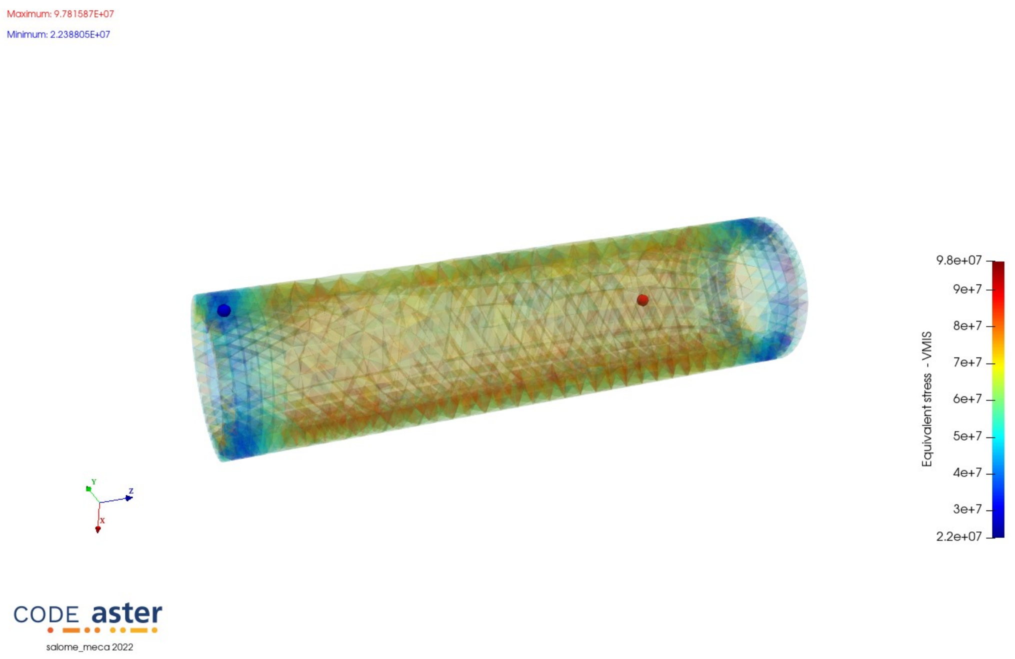

Figure 6: Maximum and minimum stress values according to the Von Mises criterion. The maximum stress value with finite elements is 9.781E7 Pa = 97.81 Mpa.

Table 2. Maximum stress values obtained by the two methods

	Theoretical (MPa)	Obtained with finite element (MPa)	Percentage error
Maximum request value	97,97	97.81	0.16 %

From the comparison of the results for the two methods used (Table 2), the theoretical one and the finite element one using Salome-Meca CODE aster software, the values differ by a very small percentage, so we can move on to checking the Stirling engine enclosure.

4.1.2 Finite Element Verification of the Stirling Engine Enclosure

The Stirling engine crankcase has a complex shape, and therefore it is necessary to use a finite element method to test the maximum working pressure values under which the external combustion engine can operate.

The first variant of the engine crankcase analyzed is shown in Figure 7.

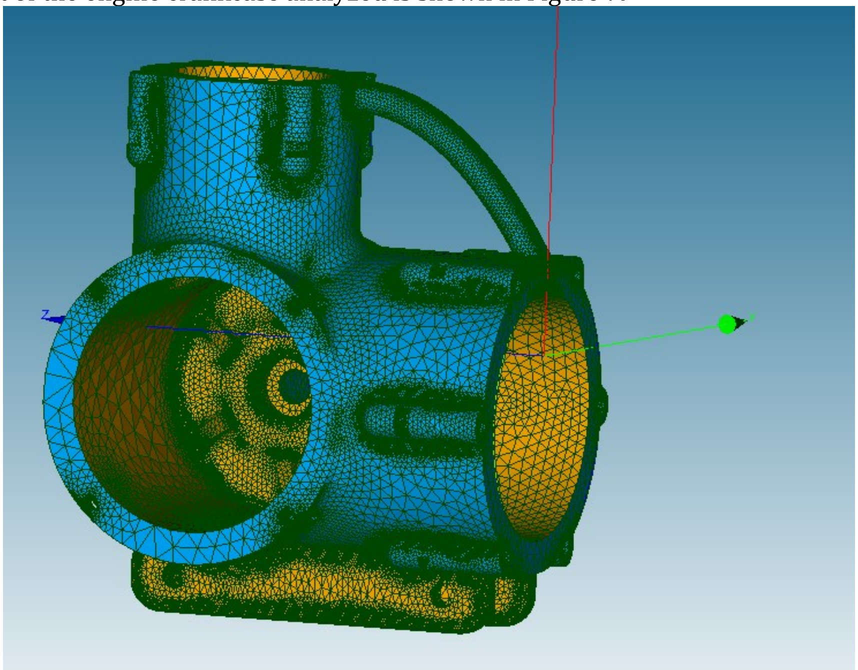

Figure 7: Variant 1 of the engine crankcase, prepared for finite element analysis

To perform the finite element analysis, zero displacement is imposed on the support surface, and various pressures are applied to the inner surface, with the resulting stress being verified for each of the applied pressures.

An Isotropic linear elasticity stress is applied with the following structure:

```
mesh = LIRE_MAILLAGE(
 FORMAT='MED',
 UNITE=20
)
model = AFFE_MODELE(
 AFFE=_F(
  MODELISATION=('3D', ),
  PHENOMENE='MECANIQUE',
  TOUT='OUI'
 ),
 MAILLAGE=mesh
)
mater = DEFI_MATERIAU(
 ELAS=_F(
  E=2575000000.0,
  NU=0.3
 )
)
materfl = AFFE_MATERIAU(
 AFFE=_F(
  MATER=(mater, ),
  TOUT='OUI'
 ),
 MODELE=model
)
mecabc = AFFE_CHAR_MECA(
 DDL_IMPO=_F(
  DX=0.0,
  DY=0.0,
  DZ=0.0,
  GROUP_MA=('Support', )
 ),
 MODELE=model
)
mecach = AFFE_CHAR_MECA(
 MODELE=model,
 PRES_REP=_F(
  GROUP_MA=('Pressiune', ),
  PRES=505000.0
 )
)
result = MECA_STATIQUE(
 CHAM_MATER=materfl,
 EXCIT=(_F(
   CHARGE=mecabc
```

```
  ), _F(
    CHARGE=mecach
  )),
 MODELE=model
)
    result = CALC_CHAMP(
 CHAM_MATER=materfl,
 CONTRAINTE=('SIGM_ELGA', 'SIGM_ELNO'),
 CRITERES=('SIEQ_ELGA', 'SIEQ_ELNO'),
 MODELE=model,
 RESULTAT=result
)
    IMPR_RESU(
 FORMAT='MED',
 RESU=_F(
  MAILLAGE=mesh,
  RESULTAT=result,
  TOUT_CHAM='OUI'
 ),
 UNITE=80
)
```

The finite element analysis is run and a graphical representation of the stresses caused by applying pressure to the inner surface is obtained. Figure 8 shows the stress generated by applying a pressure of 505000 Pa (5 atm) to the inner surface and displays the minimum and maximum stresses to which the Stirling engine body is subjected.

Finite element analyses were performed for different pressures, and the final results are presented in Table 3.

Figure 8: Representation of maximum and minimum stresses on the motor body (according to the Von Mises criterion)

Table 3. Results for variant 1 of the casing

	1	2	3	4	5
Simulation result [MPa]	25.7347	51.4649	77.2041	102.9328	128.6735
Limit Value [Mpa]	43	43	43	43	43

The imposed limit value (safety) results from the values in Table 1 and formula [9].

The graphical representation of the stresses is shown in Figure 9.

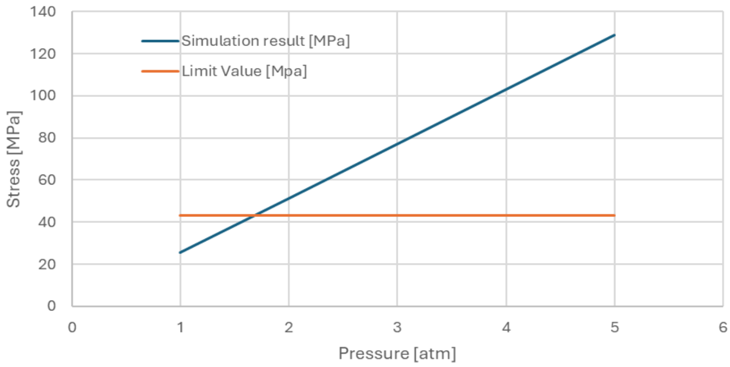

Figure 9: Numerical simulation result for housing variant 1

Figure 9 shows that the pressure can be increased to approximately 1.5 atm, and Figure 8 shows that a stress concentrator appears at one of the engine supports.

Based on these results, the Stirling engine casing is redesigned by removing the lower supports and replacing them with a side surface as shown in Figure 10.

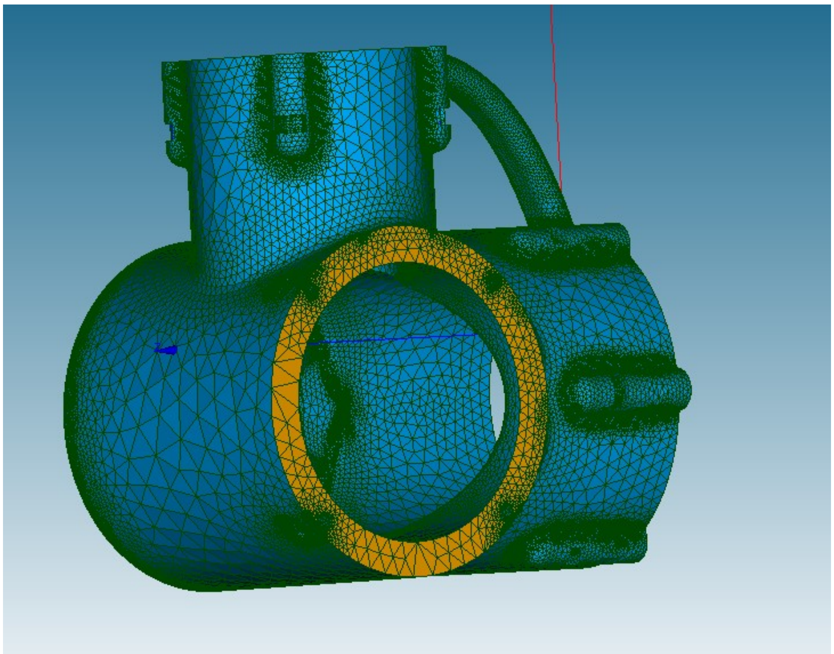

Figure 10: New base of the motor

The simulation is repeated as in the previous body variant and the following results are obtained, represented graphically in Figure 11 and numerically in Table 4:

Table 4. Simulation results for the new engine mount

Pressure [atm]	**1**	**2**	**3**	**4**	**5**	**10**	**15**	**20**
Simulation result [MPa]	3.571	7.142	13.28	15.35	17.851	35.714	53.57	71.42
Limit Value [Mpa]	43	43	43	43	43	43	43	43

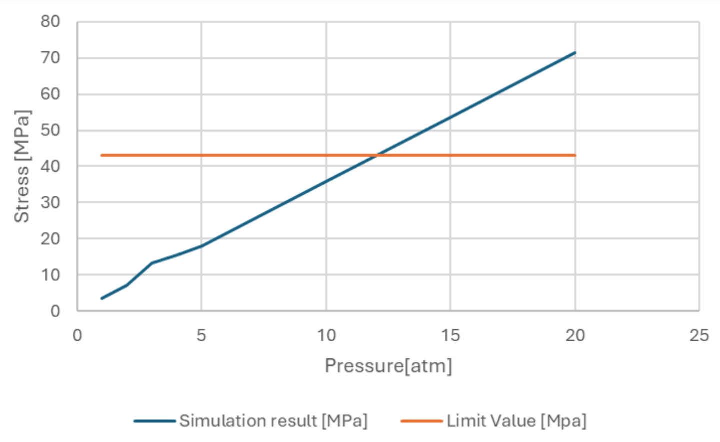

Figure 11: Stress variation for the new position of the support

From the graph resulting from the simulations (Fig. 11), the maximum pressure to which the second engine casing variant can be subjected is approximately 12 atm, which is more than 10 times higher than the first casing variant.

Figure 12 shows the positioning of the maximum and minimum positions points for the new position of the base.

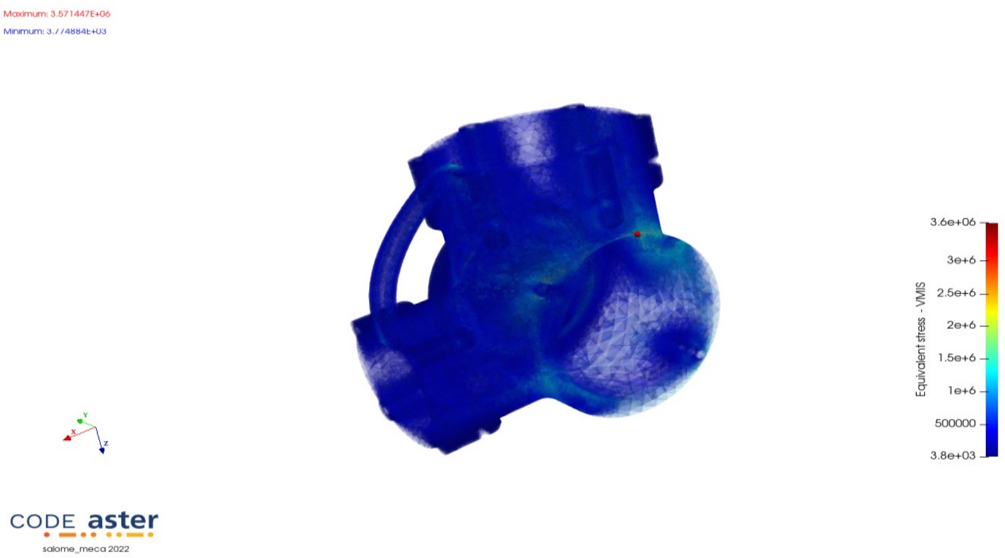

Figure 12: Position of the maximum stress on the motor enclosure for the second position of the support

5. Results and Conclusions

Following simulations and tests performed using Salome Meca software on the Stirling engine casing subjected to different pressures, it was found that the initial version with supports at the bottom introduces force concentrators that significantly reduce the strength of the analyzed part. By eliminating these concentrators and moving the engine support to a new position, an improvement of more than 10 times was achieved in the designed Stirling engine casing.

From point 4.1.1, it follows that the open source finite element testing software environment Salome-Meca offers very good analysis accuracy with very small differences between the simulation performed and the theoretical value obtained and thus by using this freely accessible finite element analysis environment, we can obtain results similar to those obtained with closed-source finite element analysis programs can be achieved and successfully can to replace expensive other finite element software from the market.

This study was conducted as part of the project "NEW TECHNIQUES AND METHODS FOR THE MANUFACTURE OF SOLAR THERMAL SYSTEMS WITH FLAT-PLATE CONCENTRATORS USING ADDITIVE MANUFACTURING METHODS" within the NUCLEU program sponsored by the Romanian Ministry of Education and Research.

References

[1] Radeș M., Rezistența materialelor, Editura Printech 2010
[2] Code_Aster / Salome-Meca - Advanced training, https://code-aster.org/spip.php?article921, october 2025
[3] Teodor M. Atanackovic, Ardeshir Guran, Theory of Elasticity for Scientists and Engineers, Springers, 2000
[4] Popescu, D. – Rezistența materialelor, vol. II, Editura Didactică și Pedagogică, București, 1983–1986
[5] Moșneagu, Gh. – Mecanică aplicată și rezistența materialelor, Editura MatrixRom, 2002.
[6] Nedelcu, D., Popovici, M. – Rezistența materialelor, Ed. Junimea, Iași.
[7] Timoshenko, S.P. & Goodier, J.N. – Theory of Elasticity, 3rd ed., McGraw-Hill, 1970.
[8] Boresi, A.P., Schmidt, R.J., Sidebottom, O.M. – Advanced Mechanics of Materials and Elasticity, 6th ed., Wiley, 2003.
[9] Ugural, A.C., Fenster, S.K. – Advanced Strength and Applied Elasticity, Pearson, 5th ed.
[10] H. Snyman, T. M. Harms, J. M. Strauss, Design analysis methods for Stirling engines, Journal of Energy in Southern Africa 19(3): 4–19, DOI: http://dx.doi.org/10.17159/2413-3051/2008/v19i3a3329
[11] Walter, Grahham - Stirling Engines, Oxford University Press, 1980, ISBN 0-19-856200-8
[12] James R. Senft – Optimum Stirling Engine Geometry, INTERNATIONAL JOURNAL OF ENERGY RESEARCH, 2002, DOI: 10.1002/er.838